Title:

Energetic Demands Regulate Sleep-Wake Rhythm Circuit Development

Authors:

Amy R. Poe[1], Lucy Zhu[1], Si Hao Tang[1], Ella Valencia[1], Matthew S. Kayser[1,2,3*]

Affiliations:

1 Department of Psychiatry, Perelman School of Medicine, University of Pennsylvania, Philadelphia, PA 19104, USA

2 Chronobiology and Sleep Institute, Perelman School of Medicine, University of Pennsylvania, Philadelphia, PA 19104, USA

3 Department of Neuroscience, Perelman School of Medicine, University of Pennsylvania, Philadelphia, PA 19104, USA

*Correspondence to: kayser@pennmedicine.upenn.edu

Abstract:

Sleep and feeding patterns lack strong daily rhythms during early life. As diurnal animals mature, feeding is consolidated to the day and sleep to the night. In *Drosophila*, circadian sleep patterns are initiated with formation of a circuit connecting the central clock to arousal output neurons; emergence of circadian sleep also enables long-term memory (LTM). However, the cues that trigger the development of this clock-arousal circuit are unknown. Here, we identify a role for nutritional status in driving sleep-wake

rhythm development in *Drosophila* larvae. We find that in the 2nd instar larval period (L2), sleep and feeding are spread across the day; these behaviors become organized into daily patterns by the 3rd instar larval stage (L3). Forcing mature (L3) animals to adopt immature (L2) feeding strategies disrupts sleep-wake rhythms and the ability to exhibit LTM. In addition, the development of the clock (DN1a)-arousal (Dh44) circuit itself is influenced by the larval nutritional environment. Finally, we demonstrate that larval arousal Dh44 neurons act through glucose metabolic genes to drive onset of daily sleep-wake rhythms. Together, our data suggest that changes to energetic demands in developing organisms trigger the formation of sleep-circadian circuits and behaviors.

Introduction

The development of behavioral rhythms such as sleep-wake patterns is critical for brain development[1]. Indeed, early life circadian disruptions in rodents negatively impacts adult behaviors, neuronal morphology, and circadian physiology[2-4]. Likewise, in humans, disruptions in sleep and rhythms during development are a common co-morbidity in neurodevelopmental disorders including ADHD and autism[5-8]. Although mechanisms encoding the molecular clock are well understood, little is known about how rhythmic behaviors first emerge[1,9-11]. In particular, cues that trigger the consolidation of sleep and waking behaviors as development proceeds are unclear[12-15].

A key potential factor in the maturation of sleep patterns is the coincident change in feeding and metabolism during development. Early in development, young animals must obtain enough nutrients to ensure proper growth[16]. Yet, developing organisms must also sleep to support nervous system development[1]. These conflicting needs

47 (feeding vs. quiescence) result in rapid transitions between sleeping and feeding states
48 early in life[17,18]. As development proceeds, nutritional intake and storage capacity
49 increase, allowing for the consolidation of feeding and sleep to specific times of day[19].
50 These changes in nutritional storage capacity are likely conserved as mammalian body
51 composition and nutritional capacity change over infant development[20] and *Drosophila*
52 show rapid increases in overall larval body size including the size of the fat body (used
53 for nutrient storage) across development[21,22]. However, the role that developmental
54 change in metabolic drive plays in regulating the consolidation of behavioral rhythms is
55 not known.

56 In adult *Drosophila*, sleep and feeding behaviors are consolidated to specific
57 times of day with flies eating more in the day than the night[23]. Yet, early in development,
58 sleep in 2nd instar *Drosophila* larvae (L2) lacks a circadian pattern[24]. We previously
59 determined that sleep-wake rhythms are initiated in early 3rd instar *Drosophila* larvae
60 (L3) (72 hr AEL). DN1a clock neurons anatomically and functionally connect to Dh44
61 arousal output neurons to drive the consolidation of sleep in L3. Development of this
62 circuit promotes deeper sleep in L3 resulting in the emergence of long-term memory
63 (LTM) capabilities at the L3 stage but not before[24].

64 Here, we identify the cues that trigger the emergence of the DN1a-Dh44 circuit
65 and the consolidation of sleep-wake rhythms in *Drosophila* larvae. We demonstrate that
66 developmental changes to energetic demands drive consolidation of periods of sleep
67 and feeding across the day as animals mature. While endogenous deeper sleep in L3
68 facilitates LTM, we find that experimentally inducing deep sleep prematurely in L2 is
69 detrimental to development and does not improve LTM performance. Additionally, we

70 demonstrate that DN1a-Dh44 circuit formation is developmentally plastic, as rearing on
71 an insufficient nutritional environment prevents establishment of this neural connection.
72 Finally, we find that Dh44 neurons require glucose metabolic genes to promote sleep-
73 wake rhythm development, suggesting that these neurons sense the nutritional
74 environment to promote circadian-sleep crosstalk.
75
76 **Results**
77 *Energetic demands limit developmental onset of rhythmic behaviors*
78 The emergence of circadian sleep-wake rhythms in *Drosophila* larvae is
79 advantageous as it enables long-term memory capabilities at the L3 stage[24]. Less
80 mature larvae (L2) do not exhibit consolidated sleep-wake patterns, prompting us to ask
81 why rhythmic behaviors do not emerge earlier in life. To determine if the absence of
82 rhythmic sleep-wake patterns in L2 might be related to feeding patterns, we examined
83 larval feeding rate (# mouth hook contractions in a 5-minute period) under constant
84 conditions at 4 times across the day (Circadian Time [CT] 1, CT7, CT13, and CT19) in
85 developmentally age-matched 2nd (L2) and early 3rd instar (L3; 72 hr AEL) larvae. While
86 we observed no differences in feeding rate across the day in L2, we found that L3 show
87 diurnal differences in feeding with higher feeding rate during the subjective day
88 compared to the subjective night (Figures 1A and 1B). Analysis of total food intake
89 indicated that L2 consume the same amount at CT1 and CT13; however, L3 at CT1
90 consume more than L3 at CT12 (Figure S1A). To assess whether the daily pattern of
91 feeding in early L3 is dependent on the canonical circadian biological clock, we
92 examined feeding rate in null mutants for the clock gene *tim*[25]. We observed no

93 differences in feeding rate across the day in L3 *tim* mutants indicating that the daily
94 feeding pattern requires a functioning molecular clock (Figure 1C). These findings
95 underscore the tight relationship between sleep and feeding across development as
96 diurnal differences in sleep emerge concurrently at the L3 stage[24].

97 To further investigate how the emergence of circadian sleep is related to
98 changes in feeding patterns during development, we asked whether enforcing a
99 constant (immature) feeding pattern at the L3 stage affects sleep-wake rhythms. First,
100 we devised a nutritional paradigm with reduced sugar content but otherwise normal food
101 (low sugar, 1.2% glucose, L.S.). Critically, this paradigm did not affect any measures of
102 larval growth or development (Figures S1D-S1F) in contrast to numerous other diets
103 that were assessed. We found that the feeding pattern in L3 raised on L.S. food closely
104 resembled that of L2 on normal food (8% glucose), with feeding spread out across the
105 day (Figure 1D) (Figure S1A). Compared to L3 raised on control food, this paradigm
106 was also associated with loss of diurnal differences in sleep duration, sleep bout
107 number, and arousal threshold (Figures 1E and 1F) (Figures S1B and S1C). Next, to
108 avoid chronic effects of this dietary manipulation, we acutely stimulated feeding in L3
109 reared on normal food using thermogenetic activation of NPF+ neurons (Figure 2A;
110 Figure S2A)[26,27]. Like L.S. conditions, enforcing a constant feeding pattern through
111 NPF+ neuron activation led to loss of sleep rhythms and loss of deep sleep in L3
112 (Figures 2B-2E; Figures S2B-S2E).

113 Disruption to circadian sleep and/or to deeper sleep stages during development
114 is associated with impairments in long-term memory formation[4,28-31]. We next asked if
115 the loss of deeper sleep observed in animals adopting an immature (constant) feeding

strategy through either the dietary paradigm or NPF+ neuron activation affects long-term memory (LTM). Consistent with deeper sleep stages being necessary for LTM, we observed a loss of LTM in either the NPF+ neuron activation (Figure 2F; Figures S2F-2I) or under L.S. conditions (Figure 2H; Figures S1G-S1I); short-term memory (STM) was intact in both manipulations (Figures 2G and 2I). These findings suggest that immature feeding strategies preclude the emergence of sleep rhythms and LTM. Together, our data indicate that consolidated periods of sleep and feeding emerge due to developmentally dynamic changes in energetic demands.

Deeper sleep stages are energetically disadvantageous in L2

To investigate if promoting deep sleep at night in L2 can enable precocious LTM abilities, we fed L2 larvae the GABA-A agonist gaboxadol[32,33]. Gaboxadol feeding effectively induced deeper sleep in L2 (as reflected by an increase in arousal threshold) although sleep duration was unchanged. Despite achieving deeper sleep, LTM was still not evident in L2 (Figures 3A,B,E; Figures S3A and S3B); however, in contrast to L3, L2 on gaboxadol failed to develop normally (Figures 3C and 3D). Next, to avoid chronic pharmacological manipulations altogether, we acutely stimulated sleep-inducing neurons using thermogenetic approaches. We found that activation of these neurons caused an increase in sleep duration and bout length with a decrease in arousal threshold (Figures 3F and 3G; Figures S3C-S3H). However, inducing deeper sleep in L2 via genetic approaches likewise did not improve LTM performance (Figure 3H; Figures S3I-S3K) despite STM being intact (Figure S3L). Moreover, as with gaboxadol feeding in L2, thermogenetic induction of deeper sleep stages disrupted larval

139 development (Figures 3I and 3J). These data suggest that sleep cannot be leveraged to
140 enhance cognitive function prematurely because prolonged periods of deep sleep are
141 not energetically sustainable at this stage.
142
143 *DN1a-Dh44 circuit formation is developmentally plastic*
144 We previously determined that Dh44 arousal neurons anatomically and
145 functionally connect to DN1a clock neurons at the L3 stage[24]. Therefore, we examined
146 the functional connectivity between clock and arousal loci in the setting of nutritional
147 perturbation by expressing ATP-gated P2X2 receptors[34] in DN1a neurons and GCaMP6
148 in Dh44 neurons. As expected, activation of DN1as in L3 raised on control food caused
149 an increase in calcium in Dh44 neurons (Figures 4A and 4B)[24]. In contrast, in L3 raised
150 on L.S. conditions, activation of DN1as no longer elicited a response in Dh44 neurons
151 (Figures 4C and 4D). Thus, the nascent connection underlying circadian sleep in
152 *Drosophila* is developmentally plastic: in an insufficient nutritional environment, this
153 connection is not functional, presumably to facilitate a more constant feeding pattern
154 that fulfills energetic needs of the animal. However, this feeding pattern eschews deep
155 sleep at the expense of LTM.
156 We previously determined that release of *CCHamide-1* (*CCHa1*) from DN1as to
157 *CCHa1mide-1 receptor* (*CCHa1-R*) on Dh44 neurons is necessary for sleep-wake
158 rhythms in L3[24]. Our data support a model in which the downstream Dh44 neurons are
159 poised to receive clock (DN1a) input as soon the connection forms between these
160 cellular populations. To test this idea directly, we next asked whether Dh44 neurons in
161 L2, before the DN1a-Dh44 connection has formed, are competent to receive the CCHa1

signal. CCHamide-1 peptide was bath applied onto dissected larval brains expressing *UAS-GCaMP7* in Dh44 neurons. As anticipated, we observed an increase in intracellular calcium in early L3 (Figure 4E); surprisingly, CCHa1 application did not alter calcium levels in Dh44 neurons in L2 (Figure 4F), indicating that Dh44 neurons are not capable of receiving CCHa1 input prior to early L3. Moreover, CCHa1 application in L3 reared on L.S. also failed to elicit a response in Dh44 neurons (Figure 4G) suggesting that sub-optimal nutritional milieu influences the development of Dh44 neuronal competency to receive clock-driven cues. Thus, our data indicate that the nutritional environment influences DN1a-Dh44 circuit development.

Dh44 neurons require glucose metabolic genes to regulate sleep-wake rhythms

How do developing larvae detect changes in their nutritional environments to drive the circadian consolidation of sleep and feeding at the L3 stage? In adult *Drosophila*, Dh44 neurons act as nutrient sensors to regulate food consumption and starvation-induced sleep suppression through the activity of both glucose and amino acid sensing genes[35-38]. We next asked whether Dh44 neurons in L3 require metabolic genes to regulate sleep-wake rhythms. In L3 raised on regular food, we conducted an RNAi-based candidate screen of different glucose and amino acid sensing genes known to act in adult Dh44 neurons. Sleep duration at CT1 and CT13 was assessed with knockdown of glucose metabolic genes (*Hexokinase-C*, *Glucose transporter 1,* and *Pyruvate kinase*) or amino acid sensing genes (*Gcn2* and its downstream target ATF4 or *cryptocephal*) in Dh44 neurons. We found that knockdown of glucose metabolism genes, *Glut1*, *Hex-C* and *PyK*, in Dh44 neurons resulted in a loss of rhythmic changes

185 in sleep duration and bout number (Figures 5A-5C; Figures S4A-S4F) with no effect on
186 L3 feeding in the *Hex-C* manipulation (Figure 5D). Manipulation of glucose metabolic
187 genes in L2 did not affect sleep duration at CT1 and CT13 (Figures 5E-5G; Figures
188 S4G-S4L) providing evidence that nutrient sensing is not required at this stage to
189 regulate sleep. In contrast to their role in adult Dh44 neurons, knockdown of amino acid
190 sensing genes, *Gcn2* and *crc*, in Dh44 neurons did not disrupt rhythmic changes in
191 sleep duration and bout number in L3 (Figures 5H and 5I; Figures S4M-S4P)
192 suggesting that Dh44 neurons may not act through amino acid sensing pathways to
193 regulate sleep-wake rhythm development. Thus, Dh44 neurons require glucose
194 metabolic genes to drive sleep-wake rhythm development. Our data indicate that the
195 emergence of daily sleep-wake patterns is regulated by developmental changes in
196 energetic capacity, and suggest that Dh44 neurons may be necessary for sensing of
197 larval nutritional environments.
198
199 **Discussion**
200 Nutritional environment and energetic status exert profound effects on sleep
201 patterns during development, but mechanisms coupling sleep to these factors remain
202 undefined. We report that the development of sleep-circadian circuits depends on
203 organisms achieving sufficient nutritional status to support the consolidation of deep
204 sleep at night. Our data demonstrate that larval Dh44 neurons act through glucose
205 metabolic genes but not amino acid sensing genes to modulate sleep-wake rhythms.
206 Larval Dh44 neurons may therefore have distinct functions from their adult counterparts
207 for integrating information about the nutritional environment through the direct sensing

208 of glucose levels to modulate sleep-wake rhythm development. Maintaining energy
209 homeostasis and sensing of the nutritional environment are likely conserved regulators
210 of sleep-wake rhythm development, as young mice exposed to a maternal low-protein
211 diet show disruptions in night-time sleep architecture and energy expenditure later in
212 life[39,40].

213 Together with our previously published work, our findings support a model in
214 which changes in both overall circuit development and molecular changes in post-
215 synaptic (Dh44) neurons likely drive sleep-wake rhythm circuit development. Our
216 CCHa1 peptide data suggest that Dh44 neurons may undergo changes in CCHa1-R
217 expression or subcellular localization between the L2 and L3 stages: we only observed
218 an increase in Dh44 neural activity in response to the bath application of CCHa1
219 peptide at the L3 stage (Figures 4E and 4F). Interestingly, this increase in activity is
220 absent in low nutrient conditions (Figure 4G) suggesting that the larval nutritional
221 environment may also modulate CCHa1-R localization or expression. Indeed, we
222 observed a disruption of sleep rhythms in L3 when glucose metabolic genes are
223 knocked down in Dh44 neurons, demonstrating that post-synaptic processes likely
224 initiate onset of circadian sleep. These findings raise intriguing questions for how
225 changes in an organism's energetic and nutritional state influence sleep-circadian circuit
226 development. Perhaps larval Dh44 neurons respond to an increase in glucose levels in
227 the environment by promoting CCHa1-R localization to the membrane. In this model,
228 changes in CCHa1-R subcellular localization allow Dh44 neurons to become competent
229 to receive clock-driven cues, while this or other Dh44-derived signals promote circuit
230 connectivity with DN1as to drive consolidation of sleep at the L3 stage. There are no

available antibodies or endogenous fluorescent reporters of CCHa1-R, limiting our ability to examine receptor subcellular localization. Nevertheless, our data open avenues for future work on the molecular and subcellular mechanisms regulating DN1a-Dh44 circuit development.

Our findings demonstrate that larvae exhibit both sleep-wake and feeding daily rhythms at the L3 stage, but not earlier[24]. This raises the obvious question of whether sleep and feeding are opposite sides of the same coin. While larvae cannot eat when they are sleeping, we have observed distinct effects of certain manipulations on sleep behaviors but not feeding. For example, knockdown of *Hex-C* in Dh44 neurons disrupts sleep rhythms with no obvious effect on feeding behavior (Figure 5D). It is, of course, possible to affect both sleep and feeding behaviors with the same manipulation (e.g., activation of NPF+ neurons) underscoring that they are highly inter-connected behaviors. Future work will leverage the larval system to examine how sleep-wake and feeding circuitry communicate to balance these rhythmic behaviors across developmental periods.

Acknowledgements:

We thank members of the Kayser Lab, Raizen Lab, and other members of the Penn Chronobiology and Sleep Institute for helpful discussions and input.

Funding:

This work was supported by NIH DP2NS111996, NIH R01NS120979, and a Burroughs Wellcome Career Award for Medical Scientists to M.S.K.; Hartwell Foundation Fellowship to A.R.P.

Author contributions:

Conceptualization, A.R.P., M.S.K.; Investigation, A.R.P., L.Z., E.V., S.H.T.; Writing – Original Draft, A.R.P. and M.S.K.; Writing – Review & Editing, all authors; Project supervision and funding, M.S.K.

Data and Materials Availability: All data needed to evaluate the conclusions in the paper are present in the paper and/or the Supplementary Materials.

Competing Interests: All authors declare that they have no competing interests.

Materials and Methods

Fly Stocks

The following lines have been maintained as lab stocks or were obtained from Dr. Amita Sehgal: iso31, tim0[25], Dh44^{VT}-Gal4 (VT039046)[41], cry-Gal4 pdf-Gal80[42], UAS-TrpA1[43], UAS-mCherry RNAi, LexAOP-GCaMP6 UAS-P2X2[34], and UAS-GCaMP7f. Dh44-LexA (80703), npf-Gal4 (25681), R76G11-Gal4 (48333), Hex-C RNAi (57404), Glut1 RNAi (40904), PyK RNAi (35218), GCN2 RNAi (67215), and crc RNAi (80388) were from the Bloomington *Drosophila* Stock Center (BDSC).

275 **Larval rearing and sleep assays**

276 Larval sleep experiments were performed as described previously[24,44]. Briefly, molting
277 2nd instar or 3rd instar larvae were placed into individual wells of the LarvaLodge
278 containing either 120 µl (for L2) or 95 µl (for L3) of 3% agar and 2% sucrose media
279 covered with a thin layer of yeast paste. The LarvaLodge was covered with a
280 transparent acrylic sheet and placed into a DigiTherm (Tritech Research) incubator at
281 25°C for imaging. Experiments were performed in the dark. For thermogenetic
282 experiments, adult flies were maintained at 22°C. Larvae were then placed into the
283 LarvaLodge (as described above) which was moved into a DigiTherm (Tritech
284 Research) incubator at 30°C for imaging.

285

286 **LarvaLodge image acquisition and processing**

287 Images were acquired every 6 seconds with an Imaging Source DMK 23GP031 camera
288 (2592 X 1944 pixels, The Imaging Source, USA) equipped with a Fujinon lens
289 (HF12.55A-1, 1:1.4/12.5 mm, Fujifilm Corp., Japan) with a Hoya 49mm R72 Infrared
290 Filter as described previously[24,44]. We used IC Capture (The Imaging Source) to acquire
291 time-lapse images. All experiments were carried out in the dark using infrared LED
292 strips (Ledlightsworld LTD, 850 nm wavelength) positioned below the LarvaLodge.

293 Images were analyzed using custom-written MATLAB software (see Churgin et al
294 2019[45] and Szuperak et al 2018[44]). Temporally adjacent images were subtracted to
295 generate maps of pixel value intensity change. A binary threshold was set such that
296 individual pixel intensity changes that fell below 40 gray-scale units within each well
297 were set equal to zero ("no change") to eliminate noise. For 3rd instars, the threshold

298 was set to 45 to account for larger body size. Pixel changes greater than or equal to
299 threshold value were set equal to one ("change"). Activity was then calculated by taking
300 the sum of all pixels changed between images. Sleep was defined as an activity value
301 of zero between frames. For 2nd instar sleep experiments done across the day, total
302 sleep was summed over 6 hrs beginning 2 hrs after the molt to second instar. For sleep
303 experiments performed at certain circadian times, total sleep in the 2nd hour after the
304 molt to second (or third) instar was summed.
305
306 **Feeding behavior analysis**
307 For feeding rate analysis, newly molted 2nd instar or 3rd instar larvae were placed in
308 individual wells of the LarvaLodge containing 120 µl of 3% agar and 2% sucrose media
309 covered with a thin layer of yeast paste. Larvae were then imaged continuously with a
310 Sony HDR-CX405 HD Handycam camera (B&H Photo, Cat. No: SOHDRCX405) for 5
311 minutes. The number of mouth hook contractions (feeding rate) was counted manually
312 over the imaging period and raw numbers were recorded. For food intake analysis,
313 newly molted 2nd instar or 3rd instar larvae were starved for 1 hr in petri dishes with
314 water placed on a Kimwipe. To compare groups of larvae of similar body weights, 13 L3
315 larvae and 26 L2 larvae were grouped together. Larvae were placed in a petri dish
316 containing blue-dyed 3% agar, 2% sucrose, and 2.5% apple juice with blue-dyed yeast
317 paste on top for 4 hrs at 25°C in constant darkness. After 4 hrs, groups of larvae were
318 washed in water, put in microtubes, and frozen at -80°C for 1 hr. Frozen larvae were
319 then homogenized in 300 µl of distilled water and spun down for 5 min at 13,0000 rpm.
320 The amount of blue dye in the supernatant was then measured using a

321 spectrophotometer (OD_{629}). Food intake represents the OD value of each
322 measurement.
323
324 **Aversive Olfactory conditioning**
325 We used an established two odor reciprocal olfactory conditioning paradigm with 10 mM
326 quinine (quinine hydrochloride, EMSCO/Fisher, Cat. No: 18-613-007) as a negative
327 reinforcement to test short-term or long-term memory performance in L2 and early L3
328 larvae[46] at CT12-15[24]. Experiments were conducted on assay plates (100 X 15 mm,
329 Genesee Scientific, Cat. No: 32-107) filled with a thin layer of 2.5% agarose containing
330 either pure agarose (EMSCO/Fisher, Cat. No: 16500-500) or agarose plus reinforcer.
331 As olfactory stimuli, we used 10 μl amyl acetate (AM, Sigma-Aldrich, Cat. No:
332 STBF2370V, diluted 1:50 in paraffin oil-Sigma-Aldrich, Cat. No: SZBF140V) and octanol
333 (OCT, Fisher Scientific, Cat. No: SALP564726, undiluted). Odorants were loaded into
334 the caps of 0.6 mL tubes (EMSCO/Fisher, Cat. No: 05-408-123) and covered with
335 parafilm (EMSCO/Fisher, Cat. No: 1337412). For naïve preferences of odorants, a
336 single odorant was placed on one side of an agarose plate with no odorant on the other
337 side. A group of 30 larvae were placed in the middle. After 5 minutes, individuals were
338 counted on the odorant side, the non-odorant side, or in the middle. The naïve
339 preference was calculated by subtracting the number of larvae on the non-odorant side
340 from the number of larvae on the odorant side and then dividing by the total number of
341 larvae. For naïve preference of quinine, a group of 30 larvae were placed in the middle
342 of a half agarose-half quinine plate. After 5 minutes, individuals were counted on the
343 quinine side, the agarose side, or in the middle. The naïve preference for quinine was

344 calculated by subtracting the number of larvae on the quinine side from the number of
345 larvae on the agarose side and then dividing by the total number of larvae. Larvae were
346 trained by exposing a group of 30 larvae to AM while crawling on agarose medium plus
347 quinine reinforcer. After 5 min, larvae were transferred to a fresh Petri dish containing
348 agarose alone with OCT as an odorant (AM+/OCT). A second group of 30 larvae
349 received the reciprocal training (AM/OCT+). Three training cycles were used for all
350 experiments. For long-term memory, larvae were transferred after training onto agarose
351 plates with a small piece of Kimwipe moistened with tap water and covered in dry active
352 yeast (LabScientific, Cat. No: FLY804020F). Larvae were then kept in the dark for 1.5
353 hrs before testing memory performance. Training and retention for thermogenetic
354 experiments were conducted at 30°C. For short-term memory, larvae were immediately
355 transferred after training onto test plates (agarose plus reinforcer) on which AM and
356 OCT were presented on opposite sides of the plate. After 5 min, individuals were
357 counted on the AM side, the OCT side, or in the middle. We then calculated a
358 preference index (PREF) for each training group by subtracting the number of larvae on
359 the conditioned stimulus side from the number of larvae on the unconditioned stimulus
360 side. For one set of experiments, we calculated two PREF values: 1a) $PREF_{AM+/OCT}$ =
361 (#AM - #OCT)/ # TOTAL; 1b) $PREF_{AM/OCT+}$ = (#OCT-#AM)/ # TOTAL. We then took the
362 average of each PREF value to calculate an associative performance index (PI) as a
363 measure of associative learning. PI = ($PREF_{AM+/OCT}$ + $PREF_{AM/OCT+}$)/2.
364
365 **Arousal threshold**

366 Blue light stimulation was delivered as described in [24,44] using 2 high power LEDs
367 (Luminus Phatlight PT-121, 460 nm peak wavelength, Sunnyvale, CA) secured to an
368 aluminum heat sink. The LEDs were driven at a current of 0.1 A (low intensity). We
369 used a low intensity stimulus for 4 sec every 2 minutes for 1 hr beginning the 2nd hr after
370 the molt to second (or third) instar. We then counted the number of larvae that showed
371 an activity change in response to stimulus. The percentage of animals that moved in
372 response to the stimulus was recorded for each experiment. For each genotype, at least
373 4 biological replicates were performed. We then plotted the average percentage across
374 all replicates.
375
376 **P2X2 Activation and GCaMP imaging**
377 All live imaging experiments (P2X2 and CCHa1 bath application) were performed as
378 described previously[24]. Briefly, brains were dissected in artificial hemolymph (AHL)
379 buffer consisting of (in mM): 108 NaCl, 5 KCl, 2 CaCl2, 8.2 MgCl2, 4 NaHCO3, 1
380 NaH2PO4-H20, 5 Trehalose, 10 Sucrose, 5 HEPES, pH=7.5. Brains were placed on a
381 small glass coverslip (Carolina Cover Glasses, Circles, 12 mm, Cat. No: 633029) in a
382 perfusion chamber filled with AHL.
383 For P2X2 imaging, dissections were performed at CT12-15 and AHL buffer was
384 perfused over the brains for 1 min of baseline GCaMP6 imaging, then ATP was
385 delivered to the chamber by switching the perfusion flow from the channel containing
386 AHL to the channel containing 2.5 mM ATP in AHL, pH 7.5. ATP was perfused for 2 min
387 and then AHL was perfused for 2 min. Twelve-bit images were acquired with a 40 X
388 water immersion objective at 256 X 256-pixel resolution. Z-stacks were acquired every 5

389 sec for 3 min. Image processing and measurement of fluorescence intensity was
390 performed in ImageJ as described previously[24]. For each cell body, fluorescence traces
391 over time were normalized using this equation: $\Delta F/F = (F_n - F_0)/F_0$, where
392 F_n=fluorescence intensity recorded at time point n, and F_0 is the average fluorescence
393 value during the 1 min baseline recording. Maximum GCaMP change ($\Delta F/F$) for
394 individual cells was calculated using this equation: $\Delta F/F_{max} = (F_{max} - F_0)/F_0$, where
395 F_{max}=maximum fluorescence intensity value recorded during ATP application, and F_0 is
396 the average fluorescence value during the 1 min baseline recording. All analysis was
397 done blind to experimental condition.
398 For CCHa1 bath application, dissections were performed at CT12-15 and AHL
399 buffer was perfused over the brains for 1 min of baseline GCaMP7f imaging, then
400 CCHa1 peptide was delivered to the chamber by switching the perfusion flow from the
401 channel containing AHL to the channel containing 1 μM synthetic CCHa1 in AHL, pH
402 7.5. CCHa1 was perfused for 2 min, followed by a 1 min wash-out with AHL. For the
403 AHL negative control, the perfusion flow was switched from one channel containing AHL
404 to another channel containing AHL. Twelve-bit images were acquired with a 40 X water
405 immersion objective at 256 X 256-pixel resolution. Z-stacks were acquired every 10 sec
406 for 4 min. Image processing and measurement of fluorescence intensity was performed
407 in ImageJ. A max intensity Z-projection of each time step and Smooth thresholding was
408 used for analysis. Image analysis was performed in a similar manner as for the P2X2
409 experiments. All analysis was done blind to experimental condition.
410
411 **Gaboxadol treatment**

412 Early second or third instar larvae were starved for 1 hour and then fed 75 µl of 25
413 mg/mL Gaboxadol (hydrochloride) (Thomas Scientific, Cat No: C817P41) in diluted
414 yeast solution for 1 hour prior to loading in LarvaLodge containing 120 µl of 3% agar
415 and 2% sucrose media covered with a thin layer of 25 mg/mL Gaboxadol yeast paste.
416 For LTM experiments, starved early second instars were fed 25 mg/mL Gaboxadol for 1
417 hour prior to training and maintained on 25 mg/mL Gaboxadol in diluted yeast solution
418 during retention period.
419

420 **Dietary Manipulations**

421 Fly food was prepared using the following recipes (based on Poe et al 2020)[47]:

Ingredients	Control food (444 mM glucose)	Low sugar (L.S.) (66 mM glucose)
Distilled H_2O	234 mL	234 mL
Agar	2 g (10g/L)	2 g (10g/L)
Glucose	20 g	3 g
Inactive yeast	20 g	20 g
Acid mix (phosphoric acid + propionic acid)	2 mL	2 mL
Target final solution volume	250 mL	250 mL

422

423 Acid Mix was made by preparing Solution A (41.5 ml Phosphoric Acid mixed with 458.5
424 ml distilled water) and Solution B (418 ml Propionic Acid mixed with 82 ml distilled
425 water) separately and then mixing Solution A and Solution B together.
426 Adult flies were placed in an embryo collection cage (Genesee Scientific, cat#: 59-100)
427 and eggs were laid on a petri dish containing either control (ctrl) or Low sugar (L.S.)
428 food. Animals developed on this media for three days.
429
430 **Larval Body Weight and Length Measurements**
431 For weight, groups of 5 early 3rd instar larvae raised on either control- or low sugar
432 (L.S.)-filled petri dishes were washed in tap water and dried using a Kimwipe. The 5
433 larvae were then weighed as a group on a scale and the weight in mg was recorded.
434 For the Gaboxadol experiments, groups of 10 early 2nd instar larvae or groups of 5 early
435 3rd instar larvae were weighed. For length, images of individual early 3rd instar larvae in
436 the LarvaLodge were measured in ImageJ (Fiji) using the straight line tool. The total
437 body length was determined in pixels for individual larvae on each condition.
438
439 **Statistical analysis**
440 All statistical analysis was done in GraphPad (Prism). For comparisons between 2
441 conditions, two-tailed unpaired *t*-tests were used. For comparisons between multiple
442 groups, ordinary one-way ANOVAs followed by Tukey's multiple comparison tests were
443 used. For comparisons between different groups in the same analysis, ordinary one-
444 way ANOVAs followed by Sidak's multiple comparisons tests were used. For
445 comparisons between time and genotype, two-way ANOVAs followed by Sidak's

446 multiple comparisons tests were used. For comparison of GCaMP signal in CCHa1

447 experiments, Mann-Whitney test was used. *P<0.05, **P<0.01, ***P<0.001.

448 Representative confocal images are shown from at least 8-10 independent samples

449 examined in each case.

450

451 **References**

452 1. Vallone, D., Lahiri, K., Dickmeis, T., and Foulkes, N.S. (2007). Start the clock!
453 Circadian rhythms and development. Dev Dyn *236*, 142-155.
454 10.1002/dvdy.20998.
455 2. Varcoe, T.J., Voultsios, A., Gatford, K.L., and Kennaway, D.J. (2016). The impact
456 of prenatal circadian rhythm disruption on pregnancy outcomes and long-term
457 metabolic health of mice progeny. Chronobiol Int *33*, 1171-1181.
458 10.1080/07420528.2016.1207661.
459 3. Mendez, N., Halabi, D., Spichiger, C., Salazar, E.R., Vergara, K., Alonso-
460 Vasquez, P., Carmona, P., Sarmiento, J.M., Richter, H.G., Seron-Ferre, M., and
461 Torres-Farfan, C. (2016). Gestational Chronodisruption Impairs Circadian
462 Physiology in Rat Male Offspring, Increasing the Risk of Chronic Disease.
463 Endocrinology *157*, 4654-4668. 10.1210/en.2016-1282.
464 4. Ameen, R.W., Warshawski, A., Fu, L., and Antle, M.C. (2022). Early life circadian
465 rhythm disruption in mice alters brain and behavior in adulthood. Sci Rep *12*,
466 7366. 10.1038/s41598-022-11335-0.
467 5. Hoffmire, C.A., Magyar, C.I., Connolly, H.V., Fernandez, I.D., and van
468 Wijngaarden, E. (2014). High prevalence of sleep disorders and associated
469 comorbidities in a community sample of children with Down syndrome. J Clin
470 Sleep Med *10*, 411-419. 10.5664/jcsm.3618.
471 6. Krakowiak, P., Goodlin-Jones, B., Hertz-Picciotto, I., Croen, L.A., and Hansen,
472 R.L. (2008). Sleep problems in children with autism spectrum disorders,
473 developmental delays, and typical development: a population-based study. J
474 Sleep Res *17*, 197-206. 10.1111/j.1365-2869.2008.00650.x.
475 7. Kotagal, S. (2015). Sleep in Neurodevelopmental and Neurodegenerative
476 Disorders. Semin Pediatr Neurol *22*, 126-129. 10.1016/j.spen.2015.03.003.
477 8. Ednick, M., Cohen, A.P., McPhail, G.L., Beebe, D., Simakajornboon, N., and
478 Amin, R.S. (2009). A review of the effects of sleep during the first year of life on
479 cognitive, psychomotor, and temperament development. Sleep *32*, 1449-1458.
480 10.1093/sleep/32.11.1449.
481 9. Carmona-Alcocer, V., Abel, J.H., Sun, T.C., Petzold, L.R., Doyle, F.J., 3rd,
482 Simms, C.L., and Herzog, E.D. (2018). Ontogeny of Circadian Rhythms and
483 Synchrony in the Suprachiasmatic Nucleus. J Neurosci *38*, 1326-1334.
484 10.1523/JNEUROSCI.2006-17.2017.

10. Sehgal, A., Price, J., and Young, M.W. (1992). Ontogeny of a biological clock in Drosophila melanogaster. Proc Natl Acad Sci U S A *89*, 1423-1427. 10.1073/pnas.89.4.1423.
11. Poe, A.R., Mace, K.D., and Kayser, M.S. (2021). Getting into rhythm: developmental emergence of circadian clocks and behaviors. FEBS J. 10.1111/febs.16157.
12. Blumberg, M.S., Seelke, A.M., Lowen, S.B., and Karlsson, K.A. (2005). Dynamics of sleep-wake cyclicity in developing rats. Proc Natl Acad Sci U S A *102*, 14860-14864. 10.1073/pnas.0506340102.
13. Blumberg, M.S., Gall, A.J., and Todd, W.D. (2014). The development of sleep-wake rhythms and the search for elemental circuits in the infant brain. Behav Neurosci *128*, 250-263. 10.1037/a0035891.
14. Frank, M.G., Ruby, N.F., Heller, H.C., and Franken, P. (2017). Development of Circadian Sleep Regulation in the Rat: A Longitudinal Study Under Constant Conditions. Sleep *40*. 10.1093/sleep/zsw077.
15. Frank, M.G. (2020). The Ontogenesis of Mammalian Sleep: Form and Function. Curr Sleep Med Rep *6*, 267-279. 10.1007/s40675-020-00190-y.
16. Ghosh, S., Korte, A., Serafini, G., Yadav, V., and Rodenfels, J. (2023). Developmental energetics: Energy expenditure, budgets and metabolism during animal embryogenesis. Semin Cell Dev Biol *138*, 83-93. 10.1016/j.semcdb.2022.03.009.
17. Adair, R.H., and Bauchner, H. (1993). Sleep problems in childhood. Curr Probl Pediatr *23*, 147-170; discussion 142. 10.1016/0045-9380(93)90011-z.
18. Levin, R., and Stern, J.M. (1975). Maternal influences on ontogeny of suckling and feeding rhythms in the rat. J Comp Physiol Psychol *89*, 711-721. 10.1037/h0077038.
19. Li, X., Zhang, C., Gong, T., Ni, X., Li, J., Zhan, D., Liu, M., Song, L., Ding, C., Xu, J., et al. (2018). A time-resolved multi-omic atlas of the developing mouse stomach. Nat Commun *9*, 4910. 10.1038/s41467-018-07463-9.
20. Toro-Ramos, T., Paley, C., Pi-Sunyer, F.X., and Gallagher, D. (2015). Body composition during fetal development and infancy through the age of 5 years. Eur J Clin Nutr *69*, 1279-1289. 10.1038/ejcn.2015.117.
21. Butterworth, F.M., Emerson, L., and Rasch, E.M. (1988). Maturation and degeneration of the fat body in the Drosophila larva and pupa as revealed by morphometric analysis. Tissue Cell *20*, 255-268. 10.1016/0040-8166(88)90047-x.
22. Jacobs, H.T., George, J., and Kemppainen, E. (2020). Regulation of growth in Drosophila melanogaster: the roles of mitochondrial metabolism. J Biochem *167*, 267-277. 10.1093/jb/mvaa002.
23. Barber, A.F., Erion, R., Holmes, T.C., and Sehgal, A. (2016). Circadian and feeding cues integrate to drive rhythms of physiology in Drosophila insulin-producing cells. Genes Dev *30*, 2596-2606. 10.1101/gad.288258.116.
24. Poe, A.R., Zhu, L., Szuperak, M., McClanahan, P.D., Anafi, R.C., Scholl, B., Thum, A.S., Cavanaugh, D.J., and Kayser, M.S. (2023). Developmental emergence of sleep rhythms enables long-term memory in Drosophila. Sci Adv *9*, eadh2301. 10.1126/sciadv.adh2301.

25. Konopka, R.J., and Benzer, S. (1971). Clock mutants of Drosophila melanogaster. Proc Natl Acad Sci U S A *68*, 2112-2116. 10.1073/pnas.68.9.2112.
26. Wu, Q., Wen, T., Lee, G., Park, J.H., Cai, H.N., and Shen, P. (2003). Developmental Control of Foraging and Social Behavior by the Drosophila Neuropeptide Y-like System. Neuron *39*, 147-161. 10.1016/s0896-6273(03)00396-9.
27. Chung, B.Y., Ro, J., Hutter, S.A., Miller, K.M., Guduguntla, L.S., Kondo, S., and Pletcher, S.D. (2017). Drosophila Neuropeptide F Signaling Independently Regulates Feeding and Sleep-Wake Behavior. Cell Rep *19*, 2441-2450. 10.1016/j.celrep.2017.05.085.
28. Konrad, C., Seehagen, S., Schneider, S., and Herbert, J.S. (2016). Naps promote flexible memory retrieval in 12-month-old infants. Dev Psychobiol *58*, 866-874. 10.1002/dev.21431.
29. Seehagen, S., Konrad, C., Herbert, J.S., and Schneider, S. (2015). Timely sleep facilitates declarative memory consolidation in infants. Proc Natl Acad Sci U S A *112*, 1625-1629. 10.1073/pnas.1414000112.
30. Jones, C.E., Opel, R.A., Kaiser, M.E., Chau, A.Q., Quintana, J.R., Nipper, M.A., Finn, D.A., Hammock, E.A.D., and Lim, M.M. (2019). Early-life sleep disruption increases parvalbumin in primary somatosensory cortex and impairs social bonding in prairie voles. Sci Adv *5*, eaav5188. 10.1126/sciadv.aav5188.
31. Smarr, B.L., Grant, A.D., Perez, L., Zucker, I., and Kriegsfeld, L.J. (2017). Maternal and Early-Life Circadian Disruption Have Long-Lasting Negative Consequences on Offspring Development and Adult Behavior in Mice. Sci Rep *7*, 3326. 10.1038/s41598-017-03406-4.
32. Dissel, S., Angadi, V., Kirszenblat, L., Suzuki, Y., Donlea, J., Klose, M., Koch, Z., English, D., Winsky-Sommerer, R., van Swinderen, B., and Shaw, P.J. (2015). Sleep restores behavioral plasticity to Drosophila mutants. Curr Biol *25*, 1270-1281. 10.1016/j.cub.2015.03.027.
33. Dijk, D.J., Stanley, N., Lundahl, J., Groeger, J.A., Legters, A., Trap Huusom, A.K., and Deacon, S. (2012). Enhanced slow wave sleep and improved sleep maintenance after gaboxadol administration during seven nights of exposure to a traffic noise model of transient insomnia. J Psychopharmacol *26*, 1096-1107. 10.1177/0269881111421971.
34. Yao, Z., Macara, A.M., Lelito, K.R., Minosyan, T.Y., and Shafer, O.T. (2012). Analysis of functional neuronal connectivity in the Drosophila brain. J Neurophysiol *108*, 684-696. 10.1152/jn.00110.2012.
35. Dus, M., Lai, J.S., Gunapala, K.M., Min, S., Tayler, T.D., Hergarden, A.C., Geraud, E., Joseph, C.M., and Suh, G.S. (2015). Nutrient Sensor in the Brain Directs the Action of the Brain-Gut Axis in Drosophila. Neuron *87*, 139-151. 10.1016/j.neuron.2015.05.032.
36. Yang, Z., Huang, R., Fu, X., Wang, G., Qi, W., Mao, D., Shi, Z., Shen, W.L., and Wang, L. (2018). A post-ingestive amino acid sensor promotes food consumption in Drosophila. Cell Res *28*, 1013-1025. 10.1038/s41422-018-0084-9.
37. Oh, Y., Lai, J.S., Min, S., Huang, H.W., Liberles, S.D., Ryoo, H.D., and Suh, G.S.B. (2021). Periphery signals generated by Piezo-mediated stomach stretch

and Neuromedin-mediated glucose load regulate the Drosophila brain nutrient sensor. Neuron *109*, 1979-1995 e1976. 10.1016/j.neuron.2021.04.028.

38. Oh, Y., and Suh, G.S.B. (2023). Starvation-induced sleep suppression requires the Drosophila brain nutrient sensor. J Neurogenet, 1-8. 10.1080/01677063.2023.2203489.

39. Sutton, G.M., Centanni, A.V., and Butler, A.A. (2010). Protein malnutrition during pregnancy in C57BL/6J mice results in offspring with altered circadian physiology before obesity. Endocrinology *151*, 1570-1580. 10.1210/en.2009-1133.

40. Crossland, R.F., Balasa, A., Ramakrishnan, R., Mahadevan, S.K., Fiorotto, M.L., and Van den Veyver, I.B. (2017). Chronic Maternal Low-Protein Diet in Mice Affects Anxiety, Night-Time Energy Expenditure and Sleep Patterns, but Not Circadian Rhythm in Male Offspring. PLoS One *12*, e0170127. 10.1371/journal.pone.0170127.

41. Jenett, A., Rubin, G.M., Ngo, T.T., Shepherd, D., Murphy, C., Dionne, H., Pfeiffer, B.D., Cavallaro, A., Hall, D., Jeter, J., et al. (2012). A GAL4-driver line resource for Drosophila neurobiology. Cell Rep *2*, 991-1001. 10.1016/j.celrep.2012.09.011.

42. Stoleru, D., Peng, Y., Agosto, J., and Rosbash, M. (2004). Coupled oscillators control morning and evening locomotor behaviour of Drosophila. Nature *431*, 862-868. 10.1038/nature02926.

43. Hamada, F.N., Rosenzweig, M., Kang, K., Pulver, S.R., Ghezzi, A., Jegla, T.J., and Garrity, P.A. (2008). An internal thermal sensor controlling temperature preference in Drosophila. Nature *454*, 217-220. 10.1038/nature07001.

44. Szuperak, M., Churgin, M.A., Borja, A.J., Raizen, D.M., Fang-Yen, C., and Kayser, M.S. (2018). A sleep state in Drosophila larvae required for neural stem cell proliferation. eLife *7*. 10.7554/eLife.33220.

45. Churgin, M.A., Szuperak, M., Davis, K.C., Raizen, D.M., Fang-Yen, C., and Kayser, M.S. (2019). Quantitative imaging of sleep behavior in Caenorhabditis elegans and larval Drosophila melanogaster. Nat Protoc *14*, 1455-1488. 10.1038/s41596-019-0146-6.

46. Widmann, A., Artinger, M., Biesinger, L., Boepple, K., Peters, C., Schlechter, J., Selcho, M., and Thum, A.S. (2016). Genetic Dissection of Aversive Associative Olfactory Learning and Memory in Drosophila Larvae. PLoS Genet *12*, e1006378. 10.1371/journal.pgen.1006378.

47. Poe, A.R., Xu, Y., Zhang, C., Lei, J., Li, K., Labib, D., and Han, C. (2020). Low FoxO expression in Drosophila somatosensory neurons protects dendrite growth under nutrient restriction. Elife *9*. 10.7554/eLife.53351.

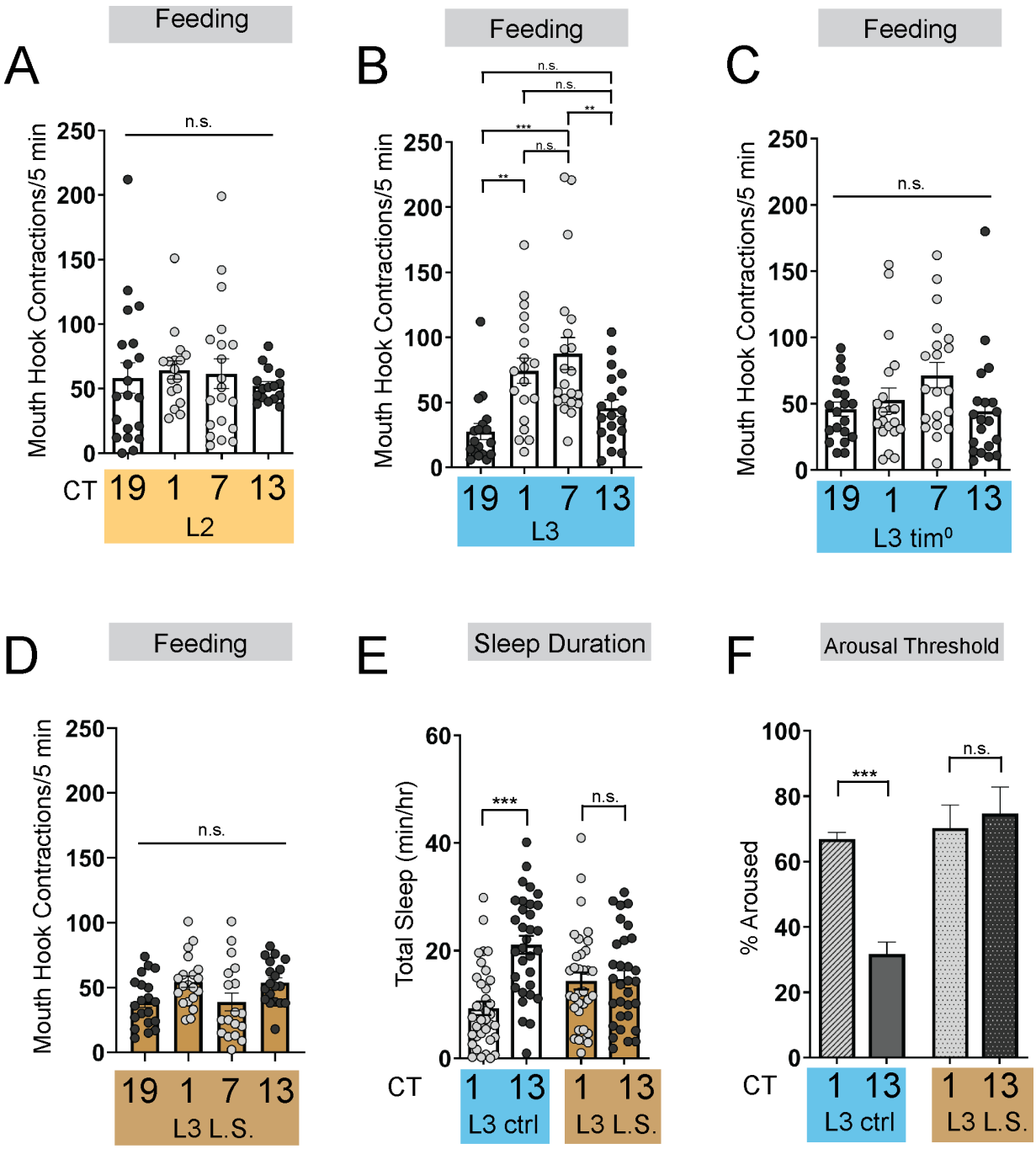

Figure 1: Energetic drive limits sleep rhythm development
(A-D) Feeding rate (# of mouth hook contractions per 5 min) of L2 controls (A), L3 raised on regular (ctrl) food (B), L3 clock mutants (C), and L3 raised on low sugar (L.S.) food (D) across the day. **(E)** Sleep duration at CT1 and CT13 in L3 raised on regular (ctrl) and L.S. food. **(F)** Arousal threshold at CT1 and CT13 in L3 raised on regular (ctrl) and L.S. food. A-D, n=18-20 larvae; E, n=29-34 larvae; F, n= n=100-172 sleep episodes, 18 larvae per genotype**.** One-way ANOVAs followed by Sidak's multiple comparisons tests [(A-D)]; Two-way ANOVAs followed by Sidak's multiple comparison test [(E-F)]. For

this and all other figures unless otherwise specified, data are presented as mean ± SEM; n.s., not significant, *$P<0.05$, **$P<0.01$, ***$P<0.001$.

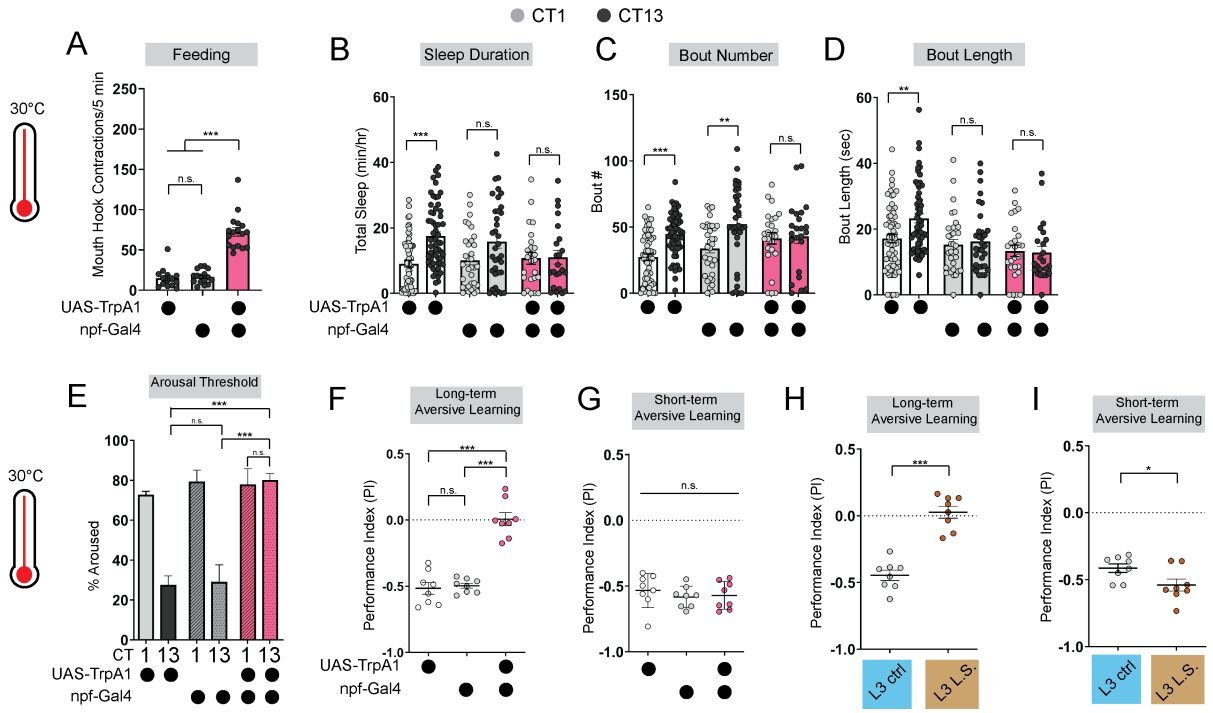

Figure 2: Immature feeding strategies limit LTM.
(A) Feeding rate of L3 expressing *npf*-Gal4>*UAS-TrpA1* and genetic controls at 30°C at CT13. **(B-D)** Sleep duration (B), bout number (C), and bout length (D) of L3 expressing *npf*-Gal4>*UAS-TrpA1* and genetic controls at 30°C. **(E-G)** Arousal threshold (E), long-term aversive memory performance (F), and short-term aversive memory performance (G) in L3 expressing *npf*-Gal4>*UAS-TrpA1* and genetic controls at 30°C. **(H,I)** Short-and long-term term aversive memory performance in L3 raised on ctrl and L.S. food. A, n=18-20 larvae; B-D, n=24-61 larvae; E, n=125-160 sleep episodes, 18 larvae per genotype; F-I, n=8 PIs (240 larvae) per genotype. One-way ANOVAs followed by Sidak's multiple comparisons tests [(A) and (E-G)]; Two-way ANOVAs followed by Sidak's multiple comparison test [(B-D)]; unpaired two-tailed Student's *t*-test [(H) and (I)].

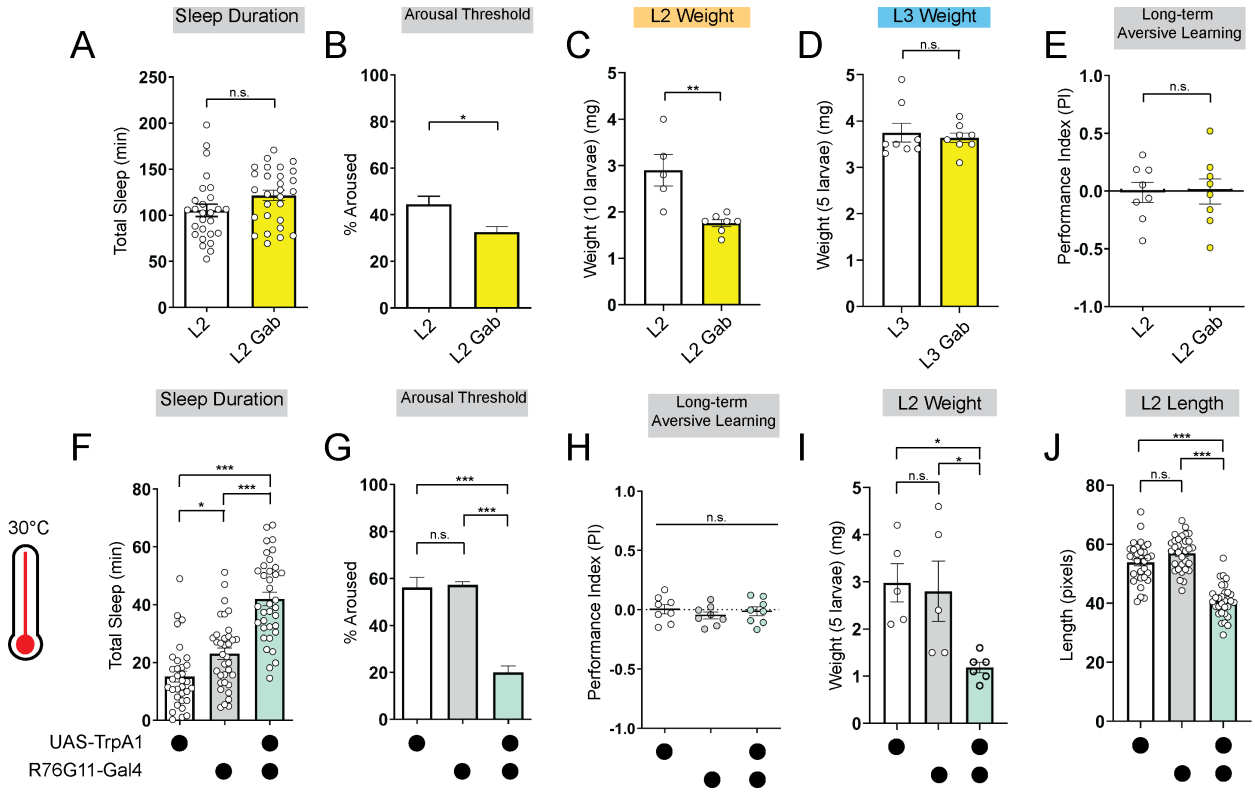

Figure 3: Deeper sleep in L2 is energetically disadvantageous.
(A, B) Sleep duration (A) and arousal threshold (B) of L2 control fed vehicle control (L2) or Gaboxadol (L2 Gab). **(C, D)** Total body weight of L2 (C) (in groups of 10) or L3 (D) (in groups of 5) fed vehicle control or Gaboxadol (Gab). **(E)** Long-term aversive memory performance in L2 fed vehicle control (L2) or Gaboxadol (L2 Gab). **(F, G)** Sleep duration (F) and arousal threshold (G) of L2 expressing *R76G11*-Gal4>*UAS-TrpA1* and genetic controls at 30°C. **(H)** Long-term aversive memory performance of L2 expressing *R76G11*-Gal4>*UAS-TrpA1* and genetic controls at 30°C. **(I, J)** Total body weight (I) and total body length (J) of L2 expressing *R76G11*-Gal4>*UAS-TrpA1* and genetic controls at 30°C. A, n=28 larvae; B, n=110-220 sleep episodes, 18 larvae per genotype; C, n=5-7 groups (50-70 larvae); D, n=8 groups (40 larvae); E, n=8 PIs (240 larvae) per genotype; F, n=33-36 larvae; G, n=234-404 sleep episodes, 30-40 larvae per genotype; H, n=8 PIs (240 larvae) per genotype; I, n=5 groups (25 larvae); J, n=31-32 larvae. Unpaired two-tailed Student's *t*-tests [(A-E)]; one-way ANOVAs followed by Sidak's multiple comparisons tests [(F-J)].

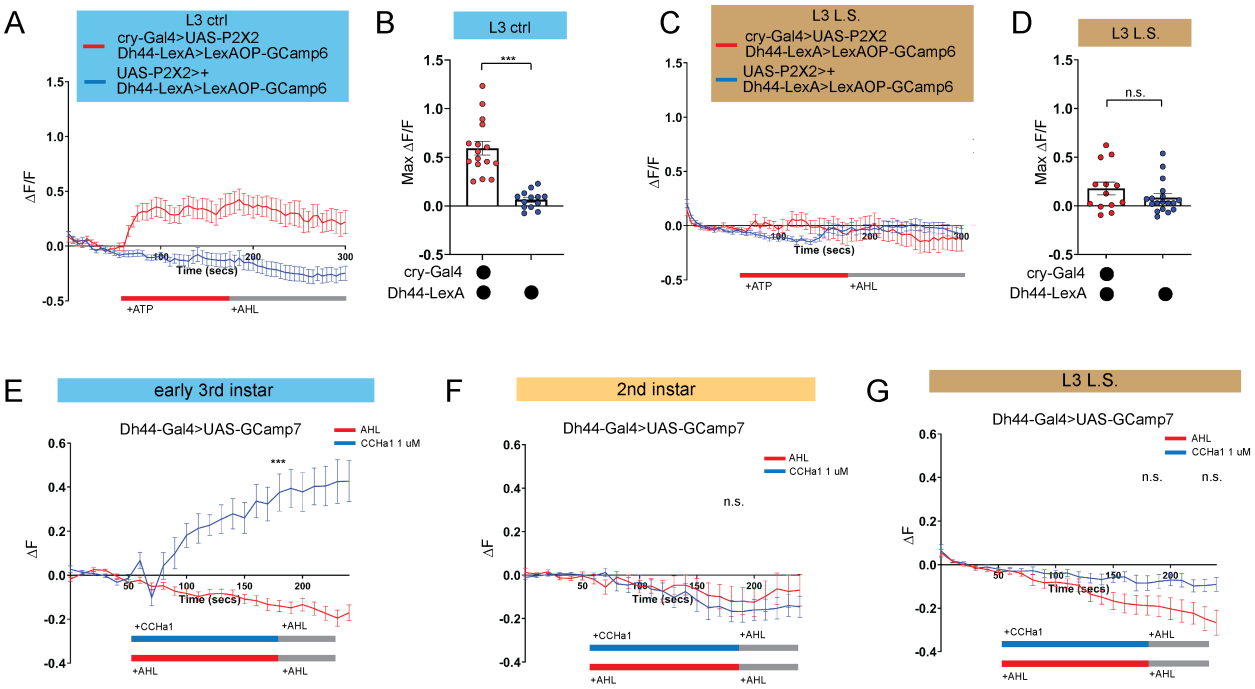

Figure 4: DN1a-Dh44 circuit formation is developmentally plastic.
(A, C) GCaMP6 signal in Dh44 neurons with activation of DN1a neurons in L3 controls (A) and L3 raised on L.S. food (C). Red bar indicates ATP application and gray bar indicates AHL application. **(B, D)** Maximum GCaMP change (ΔF/F) for individual cells in L3 controls (B) and L3 raised on L.S. food (D). **(E-G)** GCaMP7 signal in Dh44 neurons during bath application of 1 μM CCHa1 synthetic peptide in L3 controls (E), L2 controls (F) and L3 raised on L.S. food (G) brains. Red/blue bar indicates timing of CCHa1 (blue) or buffer (AHL, red) application and gray bar indicates timing of washout AHL application. A-D, n=12-18 cells, 8-10 brains; E-G, n=11-15 cells, 5-10 brains. Unpaired two-tailed Student's *t*-tests [(B) and (D)]; Mann-Whitney U test [(E-G)].

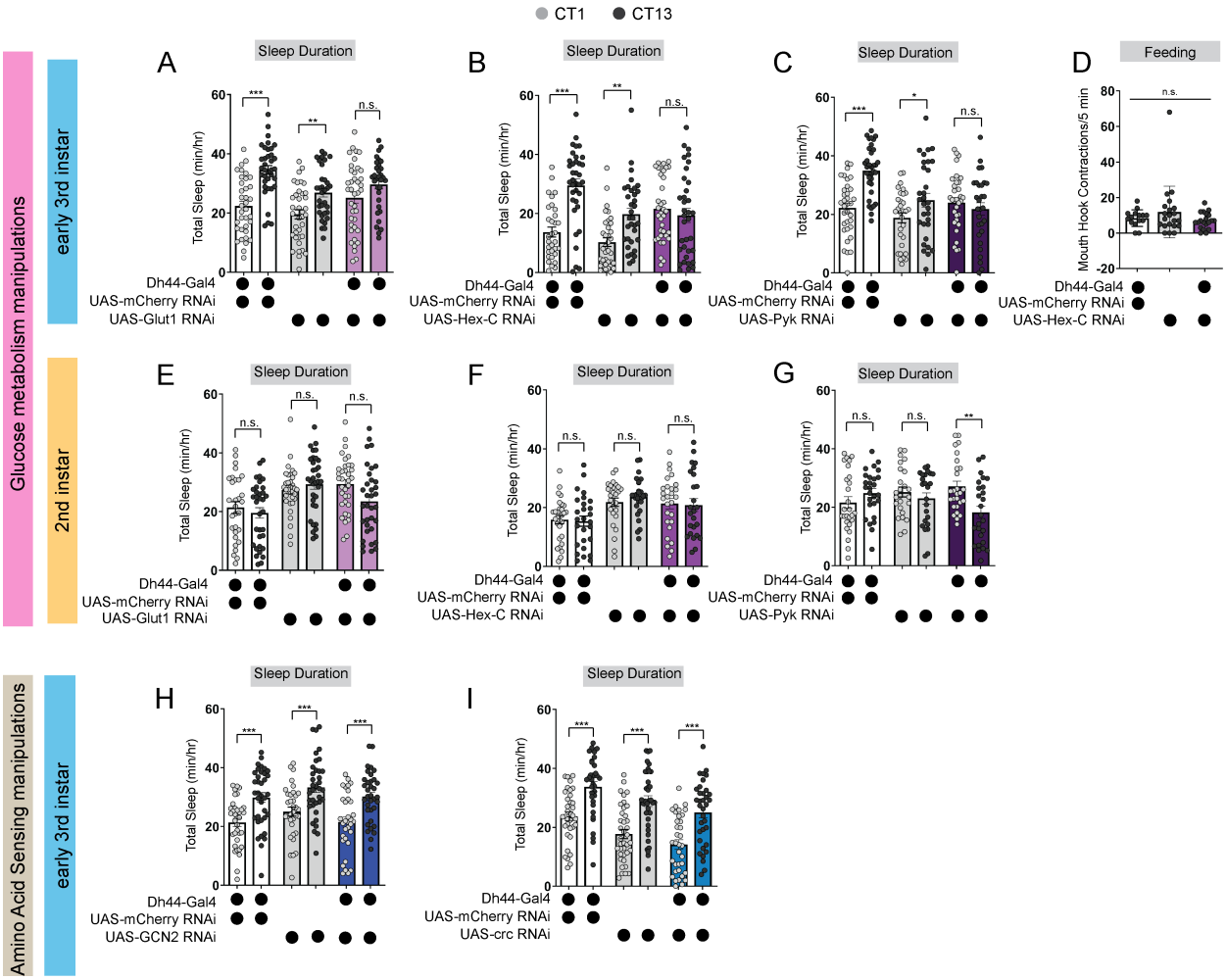

Figure 5: Dh44 neurons require glucose metabolic genes to regulate sleep-wake rhythms.

(A-C) Sleep duration in L3 expressing *UAS-Glut1-RNAi* (A), *UAS-Hex-C-RNAi* (B), and *UAS-Pyk-RNAi* (C) with *Dh44-Gal4* and genetic controls at CT1 and CT13. **(D)** Feeding rate (# of mouth hook contractions per 5 min) of L3 expressing *UAS-Hex-C-RNAi* with *Dh44-Gal4* and genetic controls at CT13. **(E-G)** Sleep duration in L2 expressing *UAS-Glut1-RNAi* (E), *UAS-Hex-C-RNAi* (F), and *UAS-Pyk-RNAi* (G) with *Dh44-Gal4* and genetic controls at CT1 and CT13. **(H, I)** Sleep duration in L3 expressing *UAS-GCN2-RNAi* (H) and *UAS-crc-RNAi* (I) with *Dh44-Gal4* and genetic controls at CT1 and CT13. A-C, n=32-40 larvae; D, n=20 larvae; E-I, n=32-40 larvae. Two-way ANOVAs followed by Sidak's multiple comparison test [(A-C) and (E-I)]; One-way ANOVAs followed by Sidak's multiple comparisons tests [(D)].

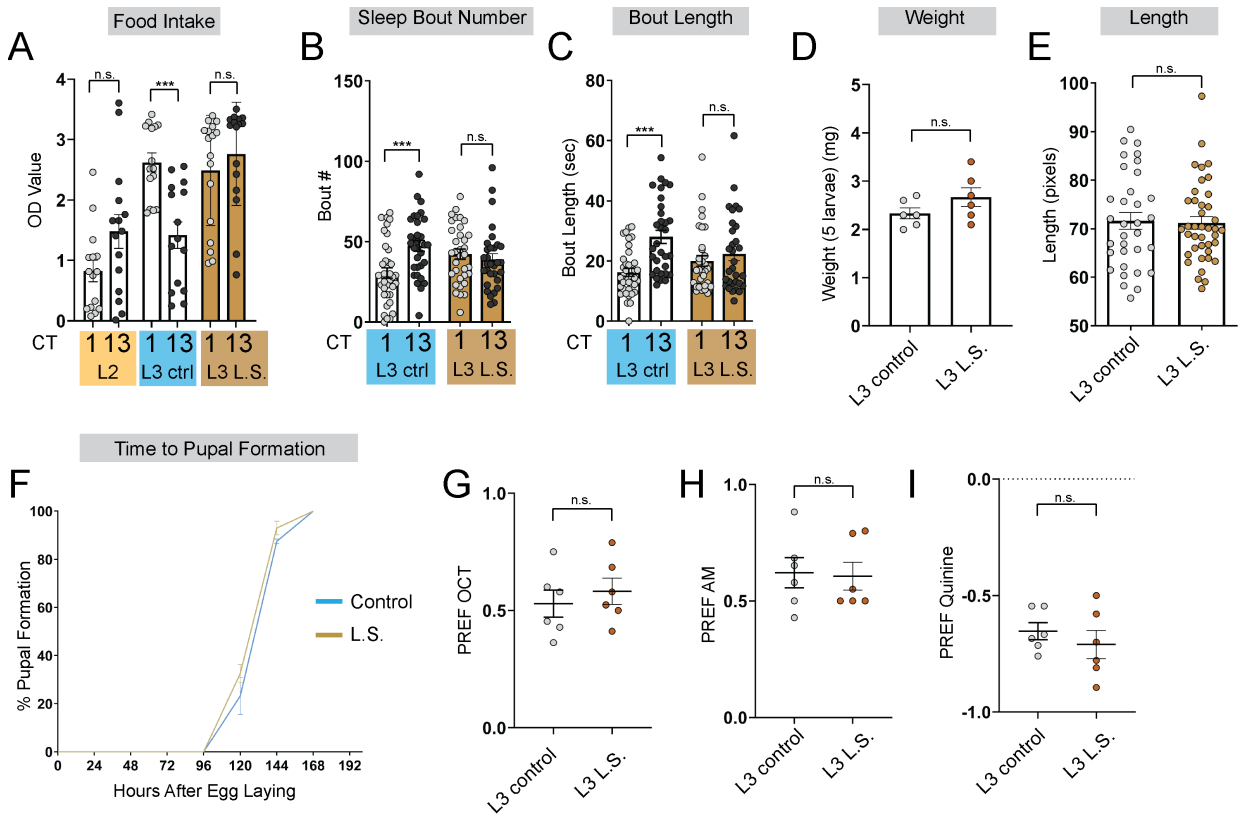

Supplemental Figure 1: Larvae reared on low sugar diet develop normally.
(A) Feeding amount of L2 controls, L3 raised on regular (ctrl) food, and L3 raised on low sugar (L.S.) food at CT1 and CT13. **(B, C)** Sleep bout number (B) and bout length (C) at CT1 and CT13 in L3 raised on regular (ctrl) and L.S. food. **(D)** Total body weight of early L3 (in groups of 5) raised on ctrl or L.S. food. **(E)** Total body length of early L3 raised on ctrl or L.S. food. **(F)** Developmental analysis of time to pupal formation of animals raised on ctrl or L.S. food. **(G-I)** Naïve OCT, AM, and quinine preference in L3 raised on ctrl and L.S. food. B-C, n=29-34 larvae; D, n=30 larvae per food condition; E, n=33-40 larvae; F, n=100-170 larvae; G-I, n=6 PREFs (180 larvae) per genotype. Two-way ANOVAs followed by Sidak's multiple comparison test [(B-C)]; Unpaired two-tailed Student's *t*-tests [(D-E) and (G-I)].

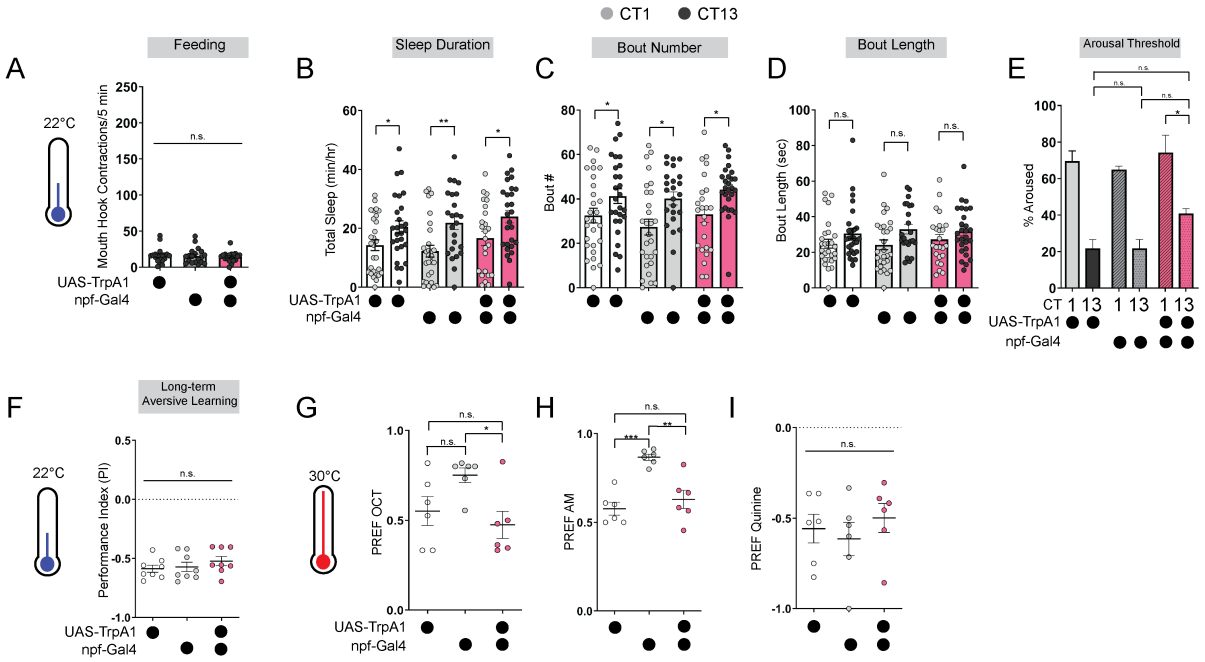

Supplemental Figure 2: Baseline odor preferences, feeding, and sleep are not affected by *npf*-Gal4 manipulations.

(A) Feeding rate of L3 expressing *npf*-Gal4>*UAS-TrpA1* and genetic controls at 22°C at CT13. **(B-E)** Sleep duration (B), bout number (C), bout length (D), and arousal threshold (E) in L3 expressing *npf*-Gal4>*UAS-TrpA1* and genetic controls at CT1 and CT13 at 22°C (temperature controls). **(F)** Long-term aversive memory performance in L3 expressing *npf*-Gal4>*UAS-TrpA1* and genetic controls at 22°C (temperature controls). **(G-I)** Naïve OCT, AM, and quinine preference in L3 expressing *npf*-Gal4>*UAS-TrpA1* and genetic controls at 30°C. A, n=18-20 larvae; B-D, n=22-27 larvae; E, n=120-205 sleep episodes, 18 larvae per genotype; F, n=8 PIs (240 larvae) per genotype; G-I, n=6 PREFs (180 larvae) per genotype. One-way ANOVAs followed by Sidak's multiple comparisons tests [(A), (E), and (F-I)]; Two-way ANOVAs followed by Sidak's multiple comparison test [(B-D)].

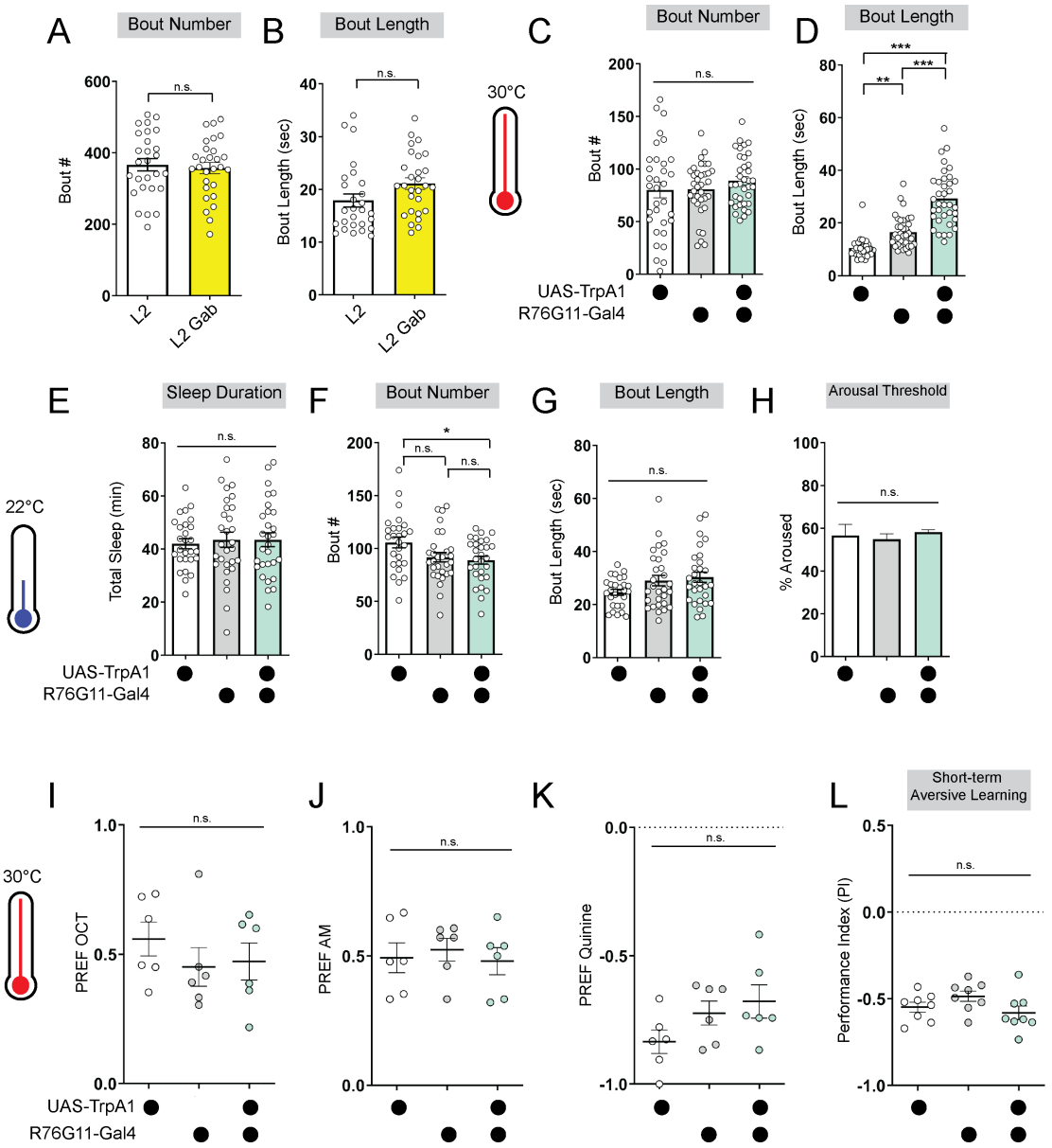

Supplemental Figure 3: Baseline sleep and odor preferences are not disrupted by *R76G11*-Gal4 manipulations.

(A, B) Sleep bout number (A) and bout length (B) of L2 control fed vehicle control (L2) or Gaboxadol (L2 Gab). **(C, D)** Sleep bout number (C) and bout length (D) of L2 expressing *R76G11*-Gal4>*UAS-TrpA1* and genetic controls at 30°C. **(E-H)** Sleep duration (E), bout number (F), bout length (G), and arousal threshold (H) of L2 expressing *R76G11*-Gal4>*UAS-TrpA1* and genetic controls at 22°C (temperature controls). **(I-K)** Naïve OCT, AM, and quinine preference in L2 expressing *R76G11*-Gal4>*UAS-TrpA1* and genetic controls at 30°C. **(L)** Short-term aversive memory performance of L2 expressing *R76G11*-Gal4>*UAS-TrpA1* and genetic controls at 30°C. A, B, n=28 larvae; C-D, n=33-36 larvae; E-G, n=27-29 larvae; H, n=145-316 sleep episodes, 30-40 larvae per genotype; I-K, n=6 PREFs (180 larvae) per genotype; L, n=8

PIs (240 larvae) per genotype. Unpaired two-tailed Student's *t*-tests [(A-B)]; One-way ANOVAs followed by Sidak's multiple comparisons tests [(C-L)].

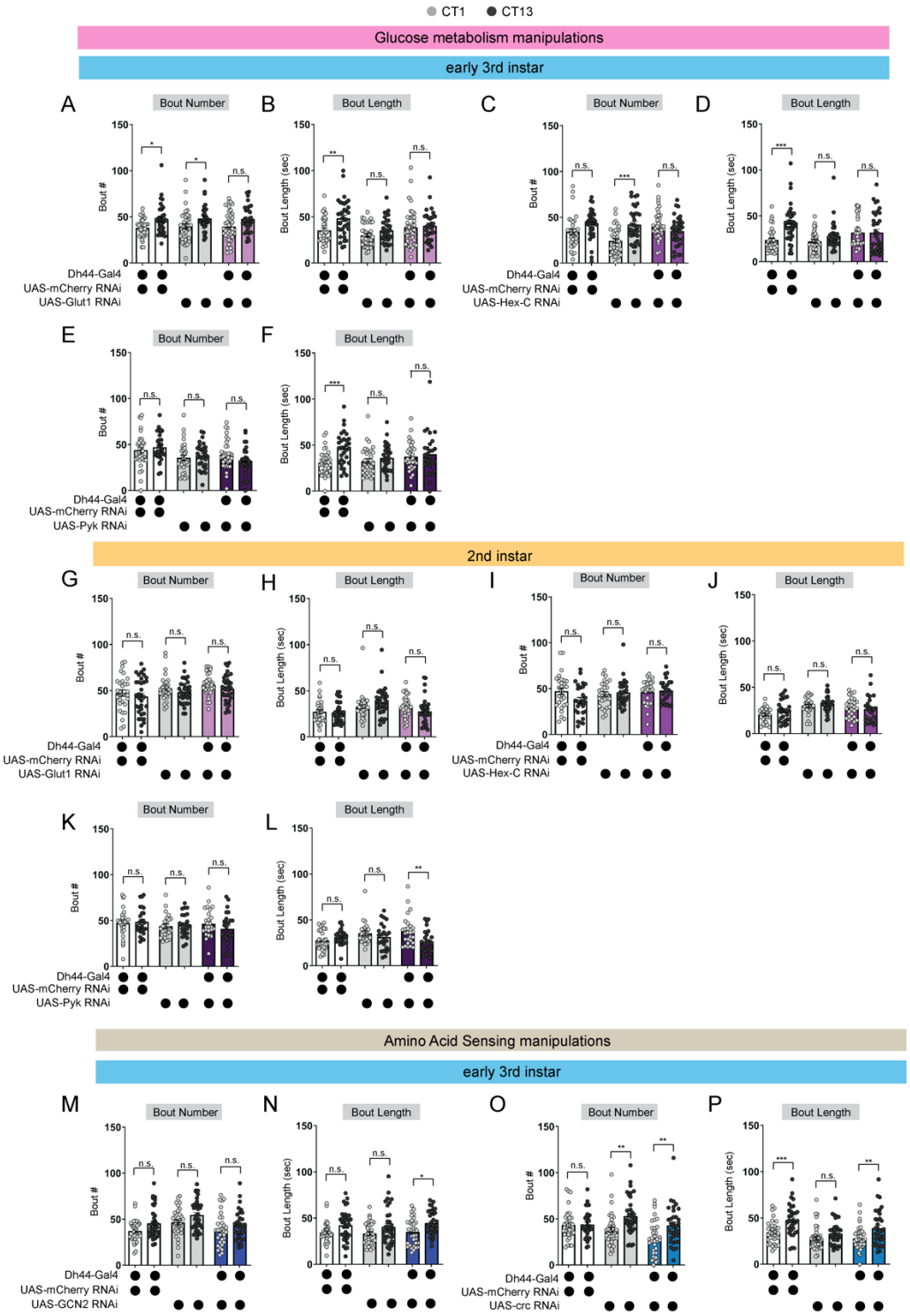

Supplemental Figure 4: Glucose metabolic gene manipulations affect L3 sleep. (A, B) Sleep bout number (A) and bout length (B) in L3 expressing *UAS-Glut1-RNAi* with *Dh44-Gal4* and genetic controls at CT1 and CT13. **(C, D)** Sleep bout number (C) and bout length (D) in L3 expressing *UAS-Hex-C-RNAi* with *Dh44-Gal4* and genetic

controls at CT1 and CT13. **(E, F)** Sleep bout number (E) and bout length (F) in L2 expressing *UAS-Glut1-RNAi* with *Dh44-Gal4* and genetic controls at CT1 and CT13. **(G, H)** Sleep bout number (G) and bout length (H) in L2 expressing *UAS-Hex-C-RNAi* with *Dh44-Gal4* and genetic controls at CT1 and CT13. **(I, J)** Sleep bout number (I) and bout length (J) in L3 expressing *UAS-GCN2-RNAi* with *Dh44-Gal4* and genetic controls at CT1 and CT13. A-J, n=32-40 larvae. Two-way ANOVAs followed by Sidak's multiple comparison test [(A-J)].